

# Engineering Assessment of Deformed Spillway Gate

David Osuna, Consulting Engineer<sup>1</sup>

<sup>1</sup>Quest Integrity NZL LTD, 69 Gracefield Rd, Lower Hutt 5010, New Zealand

## Abstract

Commissioned in 1947, Karapiro Hydro power station has a generating capacity of 96MW and is one of 9 power stations located on the Waikato River in the North Island of New Zealand. The Karapiro power station is owned and operated by Mighty River Power.

After removing the No. 2 spillway gate at Karapiro power station, it was found that the lower section of the gate had undergone permanent deformation. Corrosion on the internal and external surface of the gate was also reported. A fitness-for-service (FFS) assessment was undertaken to determine the acceptability of the spillway gate under current conditions. This paper covers the methods used to determine if the spillway gate was fit-for-continued service.

Thickness measurements were carried out on-site to determine the extent of metal loss. It was found that the metal loss magnitude was related to the location of the skinplate section with respect to the spillway gate height, where the bottom sections showed higher degrees of metal loss as compared to the top sections. An elastic-plastic stress analysis was conducted under hydrostatic operating conditions on the as-deformed gate, which included the measured corrosion damage. The stress results were computed using finite element analysis (FEA), and were used as input for the FFS assessment, and to estimate the required load for the measured deformation of the spillway gate. The acceptability of continued operation of the spillway gate was determined by satisfying the global collapse and local failure criteria found in of the ASME FFS-1 fitness-for-service standard [1].

The stress results from the FEA and the subsequent FFS assessment showed that under the current deformation and corrosion conditions, the No 2 spillway gate at Karapiro Power Station was considered fit-for-continued service. The results of the assessment allowed Mighty River Power to make an informed decision about returning the spillway gate to service.

## 1 Background

Karapiro Dam is located on the Waikato River in New Zealand and is the last dam in a series of nine on the river. The concrete arch dam is 52 m high and 335 m long. The power station which was commissioned in 1947 consists of three vertical Kaplan turbines each producing 34 MW. The station is fed from Lake Karapiro and has a nett head of 30 m.

The spillway is situated on the right abutment and consists of four gates. Each gate is 6.1 m wide and rated to 3.77 m<sup>3</sup>/s. The gates are of the Stoney roller design. Originally the gates were operated one at a time by a Goliath crane. In 1979 a dedicated winch system was installed which allows for the gates to be opened simultaneously. In 1998 the staunching bars were replaced with music note seals and the gates were reinforced for seismic events.

Late in 2014 Gate 2 was removed from service for installation of bird netting. After removing the gate, it was found that the lower section had undergone permanent deformation as seen in Figure 1. Corrosion on the internal and external surface of the spillway gate was also reported as seen on Figure 2. A fitness-for-service assessment of the current condition of the spillway gate was therefore carried out.



*Figure 1. Deflection at the bottom of spillway gate No. 2*



*Figure 2. Surface corrosion in between lower girders A3 and A2*

## 2 On-site inspection

Two on-site visits were carried out with the aim of quantifying the level of superficial corrosion through thickness measurements and identifying any modifications at present with respect to the original design of the spillway gate.

### 2.1 Thickness measurements

Thickness measurements were carried out on-site using a Panametrics 36DL-Plus UT thickness meter [2]. Thickness measurements were taken from four different locations as summarised in Table 1 and shown in Figure 3.

Table 1. Location of thickness measurement

Location	Description
A	Section in between girder A3 and A2
B	Section in between girder A2 and A1
C	Section in between girder A1 and B4
D	Section above girder B1

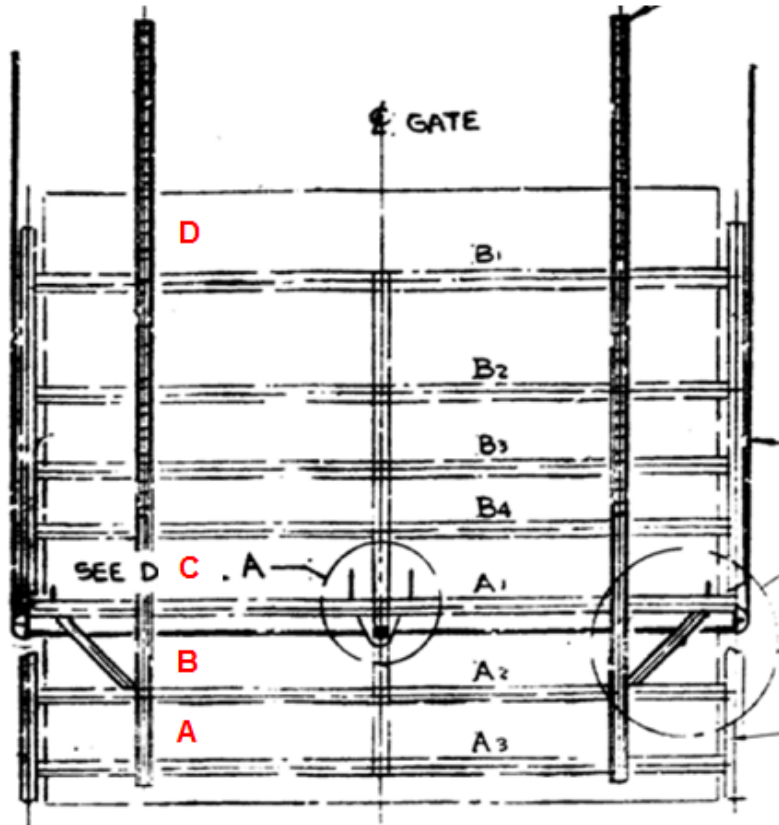


Figure 3. Location of thickness measurements readings

The readings at the four different assessed locations are summarised in Table 2.

Table 2. Thickness measurement results. Plate nominal thickness: 5/8 in (15.875 mm)

Location	Thickness readings (mm)			Min. thickness reading (mm)
A	11.42	11.36	11.71	11.36
B	13.24	13.15	13.7	13.15
C	14.63	14.68	14.9	14.63
D	15.73	15.82	15.9	15.73

Location A showed the highest level of metal loss with respect to the nominal thickness of 15.875 mm. On the other hand, location D showed minimum metal loss with a value very close to the skinplate nominal thickness. It was found that the metal loss magnitude was related to the location of the skinplate section with respect to the spillway gate height. The bottom sections showed higher degrees of metal loss compared to the top sections.

### 3 Finite Element Analysis

A finite element analysis (FEA) was undertaken with the purpose of estimating the stresses at the spillway gate due to hydrostatic loading. Two different scenarios were considered:

- a) Deformation load. Scenario to determine the possible maximum loading that caused the current deflection seen in the gate. An as-designed model with no corrosion was used.
- b) FFS requirement. Scenario to demonstrate that the current gate is fit-for-service in accordance with the plastic collapse and local failure guidelines of Annex B of ASME FFS-1. A deformed model with superficial corrosion was used.

#### 3.1 Geometry modelling

The geometry of the spillway gate was generated based on engineering drawings provided by Mighty River Power and photographic documentation taken during the on-site visit. The models were generated using the finite element modelling software Abaqus CAE 6.12-1 [3]. Two different models were generated as follows:

1. As-designed model with no corrosion.
2. Deformed model based on reported vertical deflection with superficial corrosion.

The skinplate of the spillway gate was modelled with shell elements. Similarly, beams A3, A2 and B1 were modelled using shell elements to include the connecting plates between girders A3 and A2 and the triangular reinforcement gussets of girders A3 and B1. Girders A1, B4, B3 and B2 as well as the side joists were modelled using beam elements. An overall view of the as-designed model is shown in Figure 4.

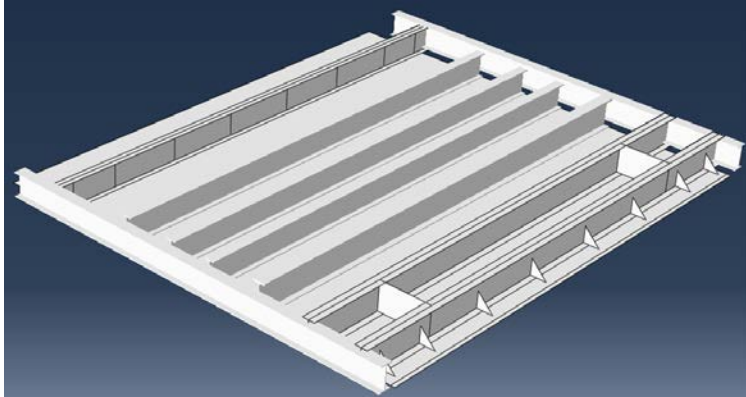


Figure 4. Overview of the spillway gate model. Connecting plates and triangular reinforcement gussets are highlighted.

The deformed model was generated based on the deflection reported by Mighty River Power at girders A3 and A4 as seen in Figure 5 and Figure 6. Only the maximum deflection point at each girder was considered to generate the deformed shape. With respect to the superficial corrosion, it was modelled by modifying the thickness of the skinplate section.

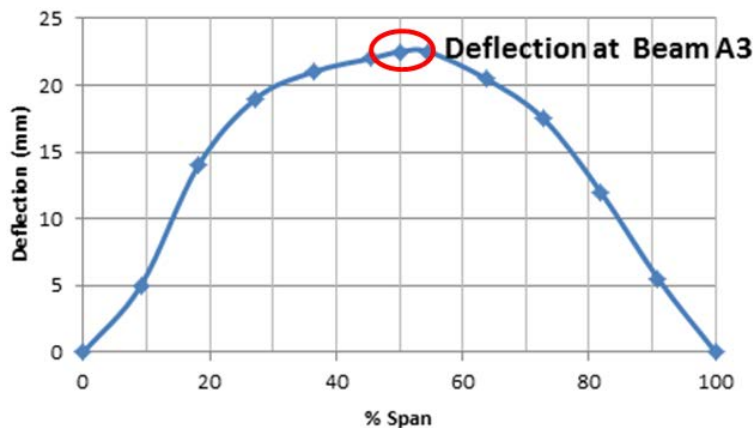


Figure 5. Measured deflection at Beam A3. Maximum deflection point is highlighted.

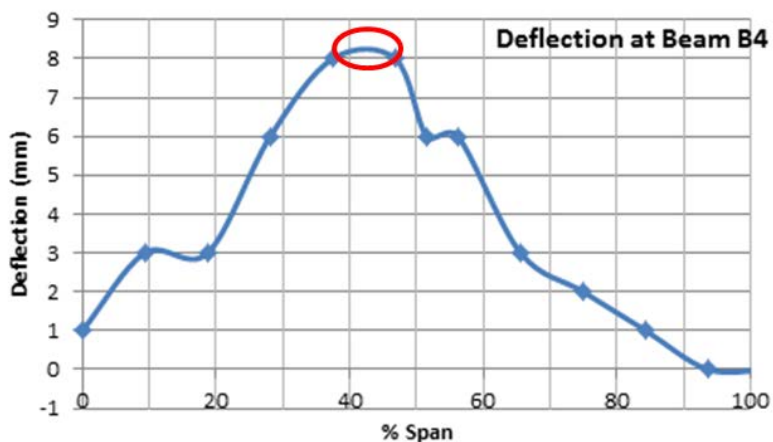


Figure 6. Measured deflection at Beam B4. Maximum deflection point is highlighted.

A function for the thickness with respect to the height of the skinplate was developed based on the on-site readings as shown in Figure 7. The height dependant function developed did not account for localised metal loss along the span of the plate; sections at the same height were considered to have the same thickness.

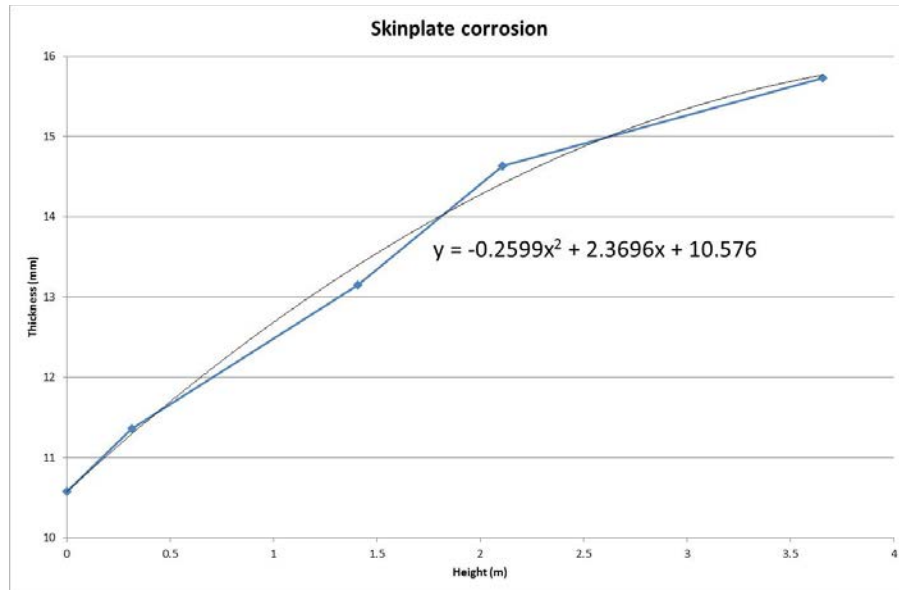


Figure 7. Analytical function used to model the superficial corrosion on the skinplate. The height-axis origin was considered to be the bottom of the spillway gate.

### 3.1.1 Geometry assumptions

In order to reduce the element number of the Finite Element model, there were features of the spillway gate that were not included as part of the modelled geometry. The following features were not included in the FE model as it was considered that they do not bear significant loading during operating conditions:

- Diagonal plate between beams A1 and A2.
- Latching racks.
- Rope retainer.
- Rope guide.
- Rope anchor bracket.

### 3.2 Model mesh

As described in section 3.1, the spillway gate was modelled using shell and beam elements. Table 3 summarises the type and number of elements used and Figure 8 shows the model mesh.

Table 3. Model mesh – Elements summary

Element type	Element specification	Number of elements
Shell	S8R: 8-node doubly curved thick shell, reduced integration	8258
	STRI65: 6-node triangular thin shell	46
Beam	B32: 3-node quadratic beam	460

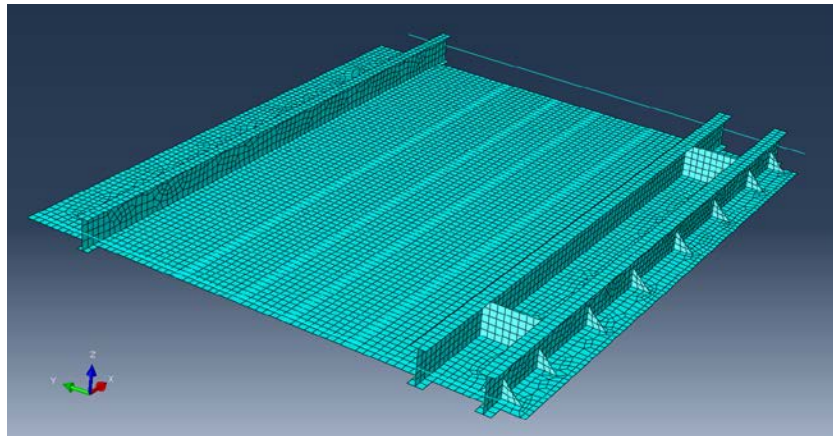


Figure 8. Spillway gate mesh.

### 3.3 Material properties

Based on engineering drawings provided by Mighty River Power, the skin plate material was specified as BS 4360:1968:Grade 43A. The minimum required tensile properties of the material are summarised in Table 4.

Table 4. BS 4360 – Grade 43A tensile properties

Material Properties	
Tensile strength	430 MPa
Yield strength	230 MPa
Elongation	20%

Elastic-plastic properties were generated based on the Ramberg-Osgood methodology in accordance with section F.2.3.2 of ASME FFS-1 using the material properties above. Figure 9 shows the true stress-strain and the engineering stress-strain curve used.

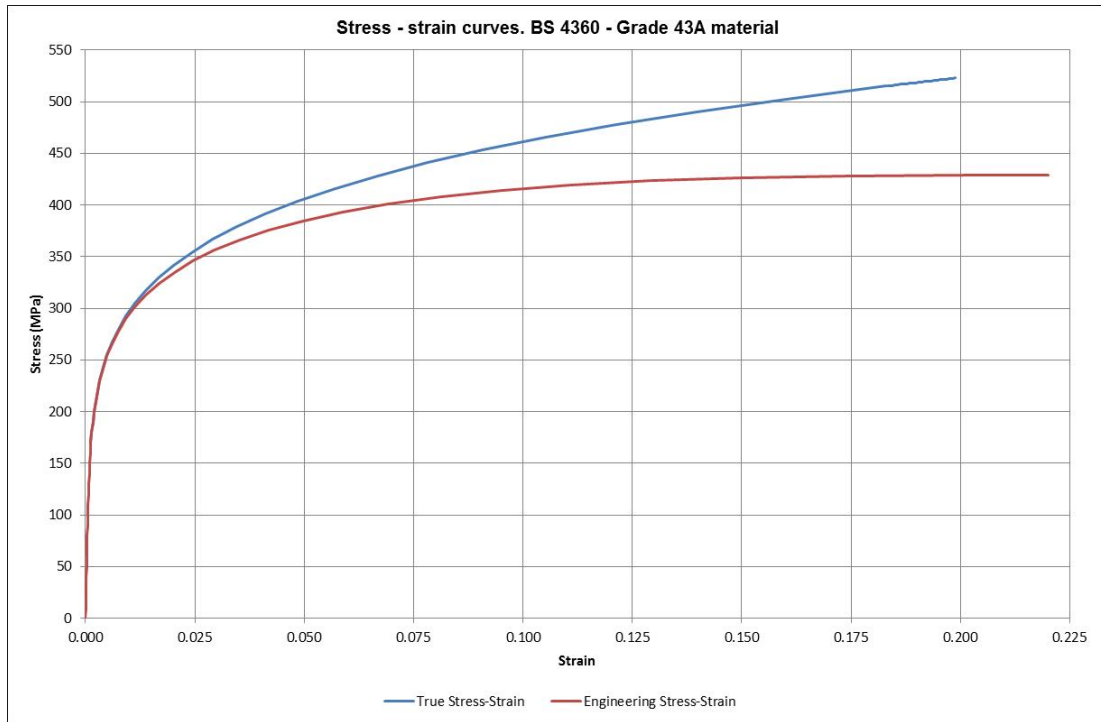


Figure 9. True stress-strain and engineering stress- strain curves. BS 4360 – Grade 43A material.

### 3.4 Loads and boundary conditions

The applied hydrostatic load to the two created models was based on a maximum operating level of 52.9 meters according to the Hydraulic Structures Hydrological Data Book as summarised in Table 5.

Table 5. Waikato Hydro System – Hydraulic Structures Hydrological Data Book

<b>Normal Operating Levels</b>	
Maximum Normal Operating Level	52.9 m
Minimum Normal Operating Level	51.5 m
Normal Operating Range	51.5 – 52.9 m
<b>Hydrological Levels</b>	
Design Flood Level	54.1 m
<b>Station Levels</b>	
Top of Spillway Gates	54.07 m

Boundary conditions were applied to the side joists to represent their interaction with the spillway gate slots. Only rotation with respect to their own axes was allowed. Figure 10 shows the hydrostatic load and the boundary conditions applied to the model.

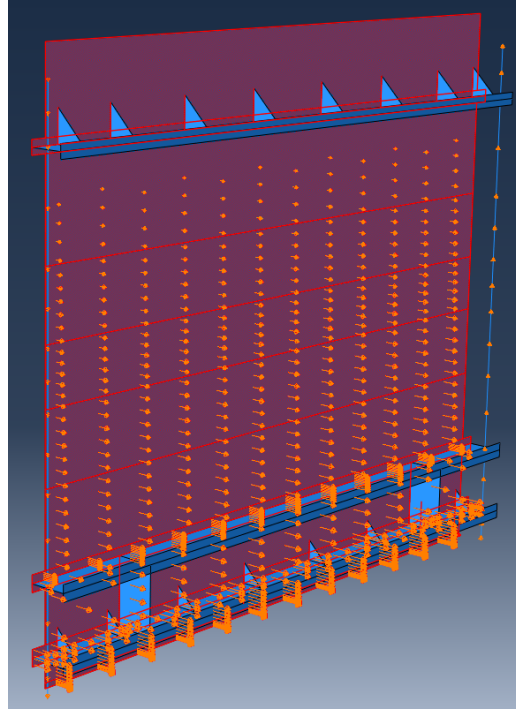
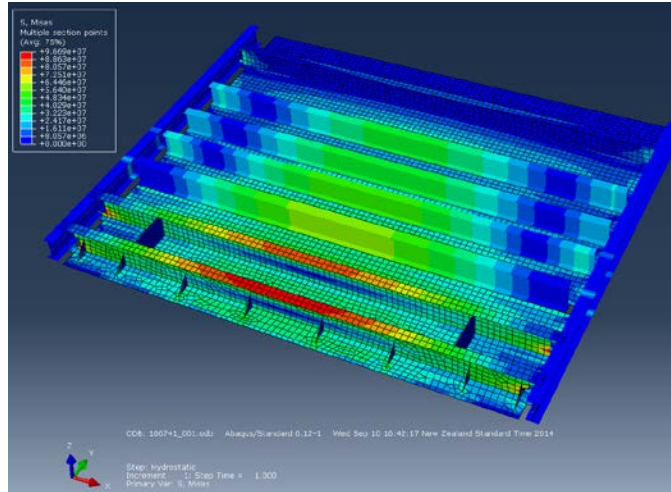


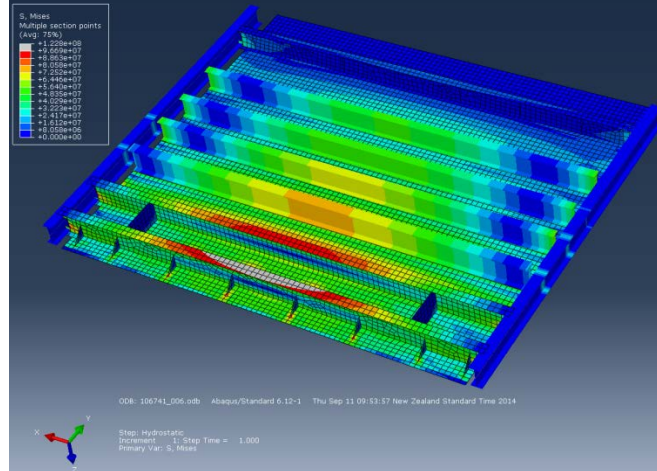
*Figure 10. Hydrostatic load and boundary conditions applied to the spillway gate model. The orange arrows represent the hydrostatic load.*

### **3.5 Stress results**

Stress results were obtained for the two different scenarios considered as described in section 3. As the hydrostatic load is highest at the bottom of the spillway gate, the highest level of stresses is seen at the bottom of the spillway gate. The locations that exhibit the highest levels of tensile stresses are the top plates of the two bottom I-beams. As seen in Figure 11, the deformed model with superficial corrosion undergoes a higher level of stresses, especially at the centre of the top plate of beam A3.



(a) As-designed model with no superficial corrosion



(b) Deformed model with superficial corrosion

Figure 11: Von Mises stress distribution under maximum operating loading conditions. Stresses in Pa.

Table 6 compares the maximum Von Mises stress values extracted from the two considered scenarios.

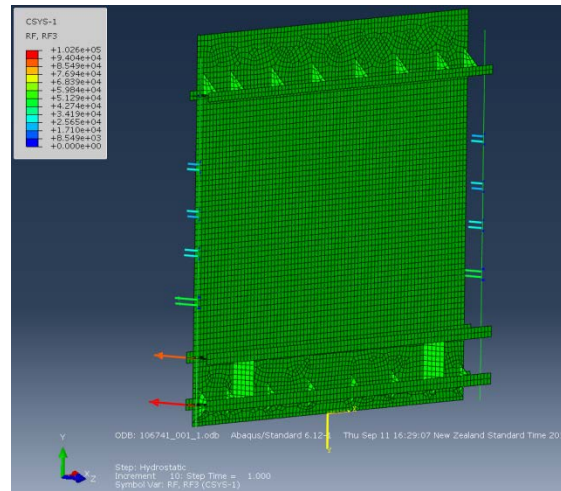
Table 6. Von Mises stresses

Finite Element model	Maximum Von Mises stress (MPa)
As-designed model with no corrosion	96.6
Deformed model with superficial corrosion	122.8

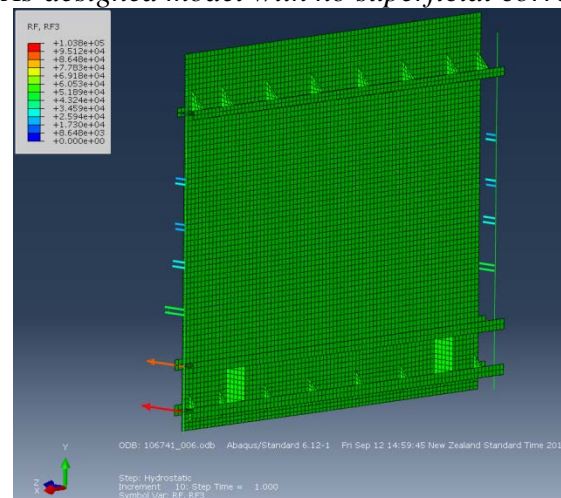
Mighty River Power requested the possible effect of the gate deformation and corrosion on its operation to be assessed. Therefore, reaction forces at the side joists were also extracted from the results for comparison purposes. Table 7 summarises the reaction values obtained from the two Finite Element Models generated. Figure 12 illustrates the direction and the magnitude of the extracted reaction forces. No significant difference in terms of reaction forces was found between the as-designed model with no corrosion and the deformed model with superficial corrosion.

Table 7. Reaction forces

Finite Element model	Maximum reaction force (N)
As-designed model with no corrosion	1.02E05
Deformed model with superficial corrosion	1.03E05



(a) As-designed model with no superficial corrosion



(b) Deformed model with superficial corrosion

Figure 12. Reaction forces to hydrostatic loading. Forces in N.

### 3.6 Deformation load estimation

The stress results were subsequently used to estimate the required load to cause the current deformation seen on the spillway gate. The process of estimating the deformation load was done in two steps:

1. Calculation of the strain that corresponds to the reported maximum vertical deflection of 23mm at beam A3.
2. Calculation of the necessary load to reach the strain level from step 1.

As seen in Figure 13, a strain of 0.13% is required to cause a vertical deformation of 23 mm at the centre of beam A3.

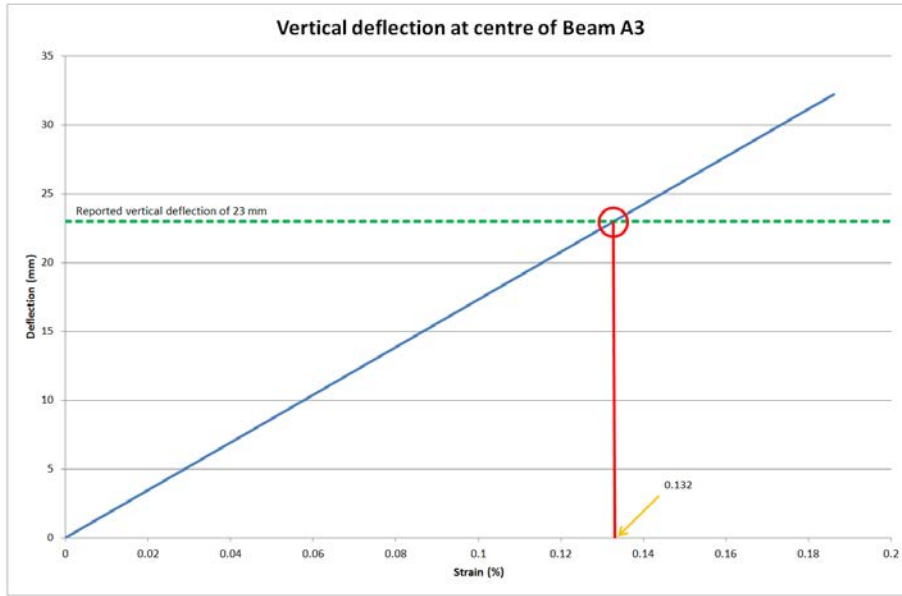


Figure 13. Vertical deflection as a function of strain. As-designed model.

For the purposes of the deformation load estimation, a load magnification factor was applied to the maximum operating load to include hydrostatic loads as big as 10 times the maximum operating load. As seen on Figure 14, to generate the plastic strain required for a vertical deflection of 23mm, a load 2.4 times the maximum operating load is required.

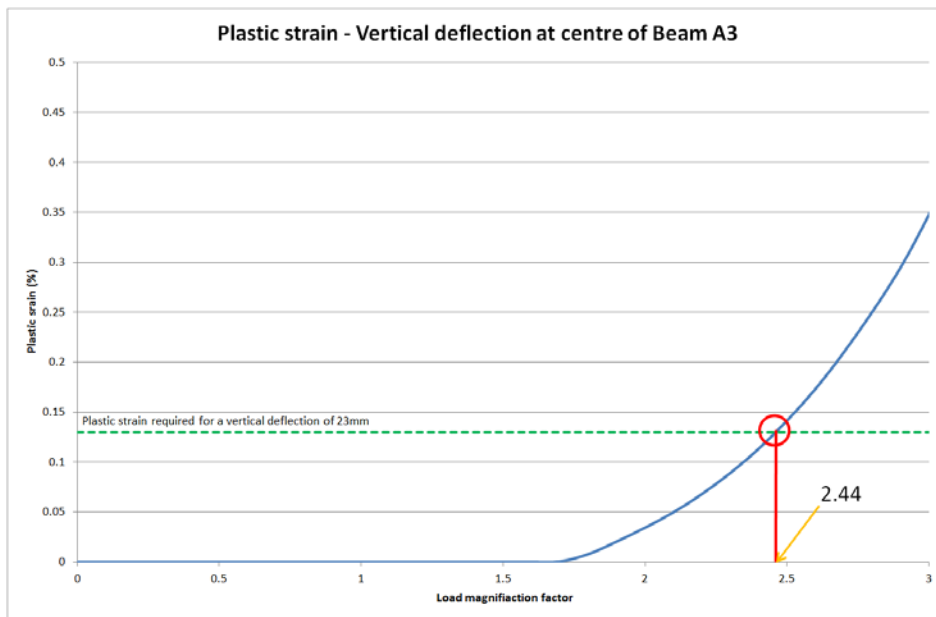


Figure 14. Plastic strain as a function of load magnification factor. As-designed model.

## 4 Fitness-for-Service assessment

To determine the acceptability of the spillway gate for protection against plastic collapse, a fitness-for-service assessment was carried out. An elastic-plastic stress analysis was undertaken on the as-deformed model with corrosion damage. The acceptability of the spillway gate using an elastic-plastic analysis was determined by satisfying the following two criteria: global collapse and local failure.

### 4.1 Global collapse criterion

To satisfy the global collapse criteria, the FE model subjected to a load factor of 3.6 is required to reach a converged solution. The load factor was determined based on the following equation, where the Remaining Strength Factor (RSF) was 0.9. The RSF is defined as the ratio of the limit load of the damaged component to the limit load of the undamaged component.

Load factor coefficient ( $\beta$ ) =  $4.0 \cdot \text{RSF}$

**Equation 1**

As seen on Figure 15, the as-deformed model of the spillway gate subjected to a load factor of 3.6 reached a converged solution. Therefore, the as-deformed model with corrosion damage satisfied the global criteria for protection against plastic collapse under the guidelines of Annex B of ASME FFS-1.

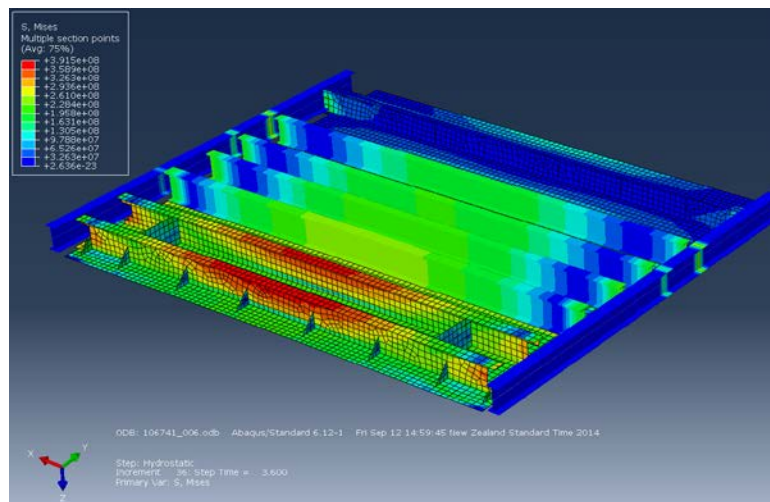


Figure 15. Von Mises distribution of the converged solution for a 3.6 load factor. Stresses in Pa.

### 4.2 Local failure criterion

In accordance with the local failure criteria guidelines of ASME FFS-1, the model that included the permanent deformation and surface corrosion is required to satisfy the failure criterion against the applied loading condition with a load factor of 1.5. High stressed locations were identified for the assessment and assessed as seen in Figure 16 for that particular loading scenario.

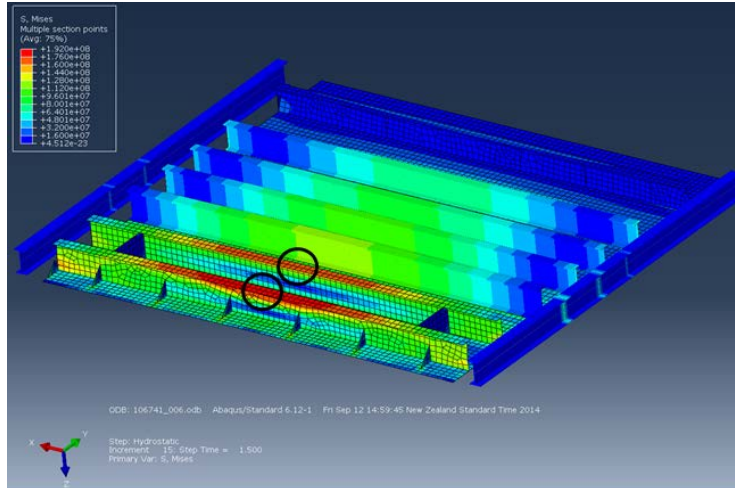


Figure 16. Von Mises stress distribution. Load factor of 1.5. The two locations assessed for local failure are indicated. Stresses in Pa.

For the component to satisfy the local failure criterion, the total equivalent plastic strain ( $\epsilon_{peq}$ ) must be less than the limiting triaxial strain ( $\epsilon_L$ ). The total equivalent plastic strain at the assessed locations is extracted from the results of the elastic-plastic analysis with the load factor of 1.5. A distribution of the total equivalent plastic strain is shown in Figure 17.

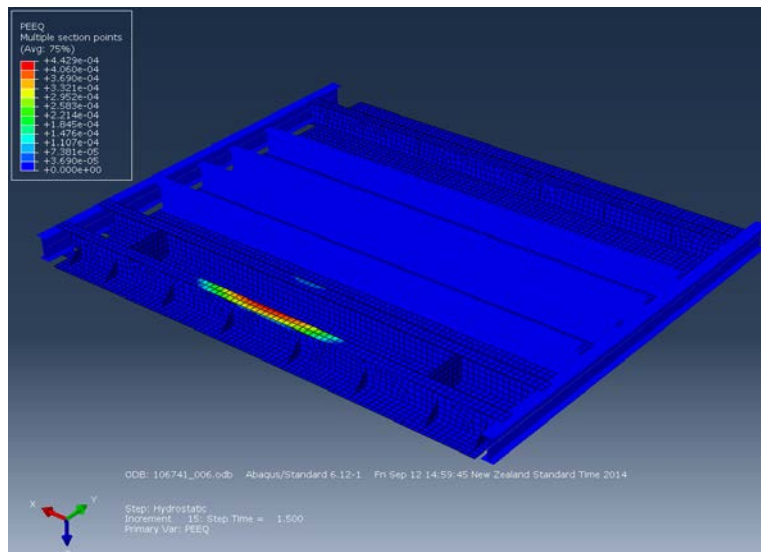


Figure 17. Equivalent plastic strain. Load factor of 1.5.

The limiting triaxial strain is calculated based on the guidelines provided Annex B of ASME FFS-1, following Equation 2 as shown on Table 8.

$$\epsilon_L = \epsilon_{Lu} \cdot \exp \left[ - \left( \frac{\alpha_{sl}}{1+m_2} \right) \left( \left\{ \frac{(\sigma_1 + \sigma_2 + \sigma_3)}{3\sigma_e} \right\} - \frac{1}{3} \right) \right]$$

Equation 2

Table 8. Limiting triaxial strain – assessed location at beams A3 and A2

Parameters for local failure criterion	
Yield Strength (MPa)	230
Ultimate Tensile Strength (MPa)	430
Elongation (%)	22
YS / UTS ratio	0.534884
Strain hardening exponent: $m_2$	0.27907
Elongation specified	0.3977
Uniaxial strain limit: $\epsilon_{Lu}$	0.3977
$\alpha_{sl}$	2.2
Principal stress in the X-direction: $\sigma_1$ (MPa)	187
Principal stress in the Y-direction: $\sigma_2$ (MPa)	0.50
Principal stress in the Z-direction: $\sigma_3$ (MPa)	0
Von Mises Stress: $\sigma_e$ (MPa)	187
Limiting triaxial strain: $\epsilon_L$	0.397

The results of the assessment are summarised in Table 9.

Table 9. Local failure criteria

Location	Centre of A3 beam	Centre of A2 beam
Limiting triaxial strain, $\epsilon_L$	0.397	0.397
Total eq. plastic strain, $\epsilon_{peq}$	0.044	0.005
Is $\epsilon_{peq} < \epsilon_L$ ?	PASS	PASS

Figure 18 shows a plot of the criticality of locations for the local failure criterion by displaying the total equivalent plastic strain – triaxial strain limit ratio. As all the areas show a ratio below 1, it is considered that the spillway gate satisfies the local failure criterion. However, it was determined that under the current levels of deformation and metal loss, the most critical location corresponds to the top plate at the centre of beam A3.

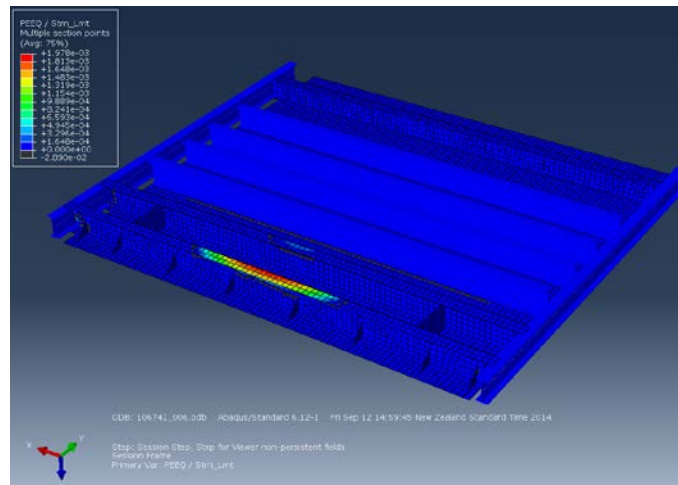


Figure 18. Plot of the Eq. Plastic strain – Triaxial strain limit ratio. Load factor of 1.5.

## **5 Conclusions**

Based on the results of the Level 3 Fitness-for-Service assessment, the following was concluded:

- Under its current conditions, Spillway gate No 2 at Karapiro Power Station is considered to be fit-for-service as it has met the global collapse and local failure requirements under the guidelines of Annex B of ASME FFS-1.

## 6 References

1. The American Petroleum Institute and The American Society of Mechanical Engineers, Fitness-for-Service API 579/ASME FFS-1 (API 579 Second Edition). © API Publishing Services June 5, 2007.
2. Panametrics 36DL-Plus UT thickness meter. Panametrics, Inc. NDT Division. USA.
3. Abaqus CAE 6.12-1. Dassault Systèmes Simulia Corp., Providence, RI, USA.

## **The Author**

**David Osuna** is a consulting engineer with 9 years' experience in stress analysis, Fitness-for-Service assessments and asset integrity management. He holds a bachelor's degree in Mechanical Engineering and a Masters of Business Administration from Victoria University of Wellington. David is part of the Quest Integrity Structural Integrity Team. He has carried out comprehensive fitness-for-service assessments for numerous components in the oil, gas and power industries following the guidelines of standards such as ASME FFS-1 and BS7910. He works closely with hydro power operators in New Zealand during the recommissioning and refurbishment process and has recently worked alongside a major hydro power company in assessing critical hydro equipment currently under refurbishment.